THE DEVELOPMENT OF A MEASUREMENT CHAIN FOR THE MONITORING AND ANALYSIS OF POLYMER MACHINING

B. Aldwell[1], R. Hanley[2], G. E. O'Donnell[1]

1. Department of Mechanical & Manufacturing Engineering, Trinity College Dublin, Dublin 2, Ireland.
2. DePuy Ireland, Loughbeg, Ringaskiddy, Co Cork, Ireland.

ABSTRACT

The machining of polymers is an area which is not well understood. Most polymer machining is undertaken under the assumption that it is valid to use tooling and machining parameters which have been designed for the machining of alloys. This assumption is often shown to be invalid, as it ignores the time and temperature dependent viscoelastic behaviour of polymers, and their unique chip formation mechanisms. The result of this assumption is often that machining is carried out under suboptimal conditions, causing poor surface finish, poor dimensional accuracy, and undesired burr formation. In an industrial setting this causes rejected products, leading to increased waste and reduced productivity.

In order to effectively characterise the machining of polymers, an extensive measurement chain is required. This measurement chain must collect data on cutting forces, cutting temperatures, chip formation mechanisms, and surface roughness of finished parts. In addition, the tool used must be characterised, through measurement of rake angle, edge radius/sharpness, and surface roughness of the rake face. The data collected must then be processed in order to allow meaningful conclusions to be made from the experiments conducted. This paper details the development of a measurement chain to meet these requirements.

KEYWORDS: Polymer, Machining, Monitoring

1. INTRODUCTION

Polymers are extremely versatile materials with a wide variety of applications, such as use in orthopaedic implants for total knee replacements, as shown in Figure 1. While traditional polymer processing techniques are well understood, there are some applications where surface roughness and dimensional accuracy requirements call for further finishing operations, such as machining.

There is little information available on the machining of polymers, with much of the knowledge of suitable machining parameters being proprietary [1]. As a result, cutting conditions designed for metal cutting are often used, with suboptimal results. The first work to acknowledge that the machining of polymers is fundamentally different from that of metals was authored by Kobayashi [2, 3] in the 1960s. Kobayashi measured cutting forces over a range of rake angles, and characterised the types of chip formation experienced when machining polymers. His later work involved stress intensity factors [4], crack propagation [5-10] and creep behaviour in polymers [11].

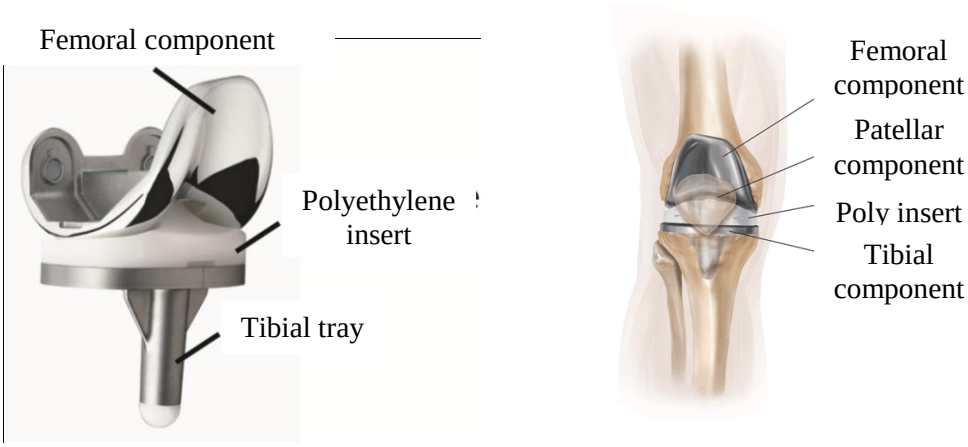

Figure 1: Knee prosthesis system (left), and illustration of implant in service (right)

One of the main challenges in the machining of polymers is the viscoelastic nature of the stress-strain relationship [12], which is dependent on both time/strain rate and temperature [13, 14]. This complex behaviour leads to unique chip formation mechanisms [3, 15, 16], and to problems with viscous deformation of the workpiece, which can cause dimensional accuracy issues when machining. Kobayashi identified the concept of a critical rake angle [17], where the thrust force into/out of the workpiece is zero. At this rake angle, which is unique for each set of cutting conditions, deformation of the workpiece is minimised. This deformation is illustrated in Figure 2, with the high rake angle shown in (a) having far less deformation than the negative rake angle shown in (c).

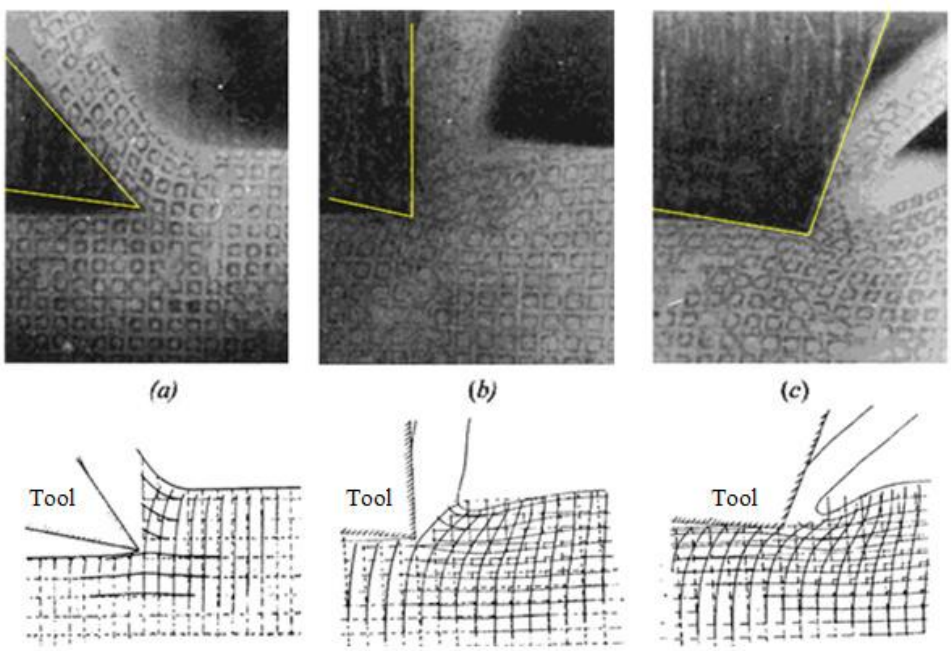

Figure 2: Deformation of workpiece for a range of rake angles [2]

As part of his work Kobayashi published a table of factors and their effects, part of which is reproduced in Table 1.

Factor	Has major effect on
Tool	
Rake angle	Chip formation
Point Radius	Roughness of cut surface
Machining conditions	
Depth of cut	Chip formation and roughness of cut surface
Cutting speed	

Table 1: Factors and their effects [2]

While this table notes the factors involved, it does not give a measure of their relative importance, or the exact nature of their effect on the machining operation. It is clear that fundamental work is required to quantify the exact nature of these effects, thus facilitating the selection of better machining conditions. In order for this work to be undertaken a suitable experimental setup and measurement chain must first be developed [18].

2. DEVELOPMENT OF MEASUREMENT CHAIN

2.1 Methodology

The experimental methodology shown in Figure 3 was applied. This paper concentrates on the development of the in process measurement chain, with the addition of chip analysis and surface roughness measurements.

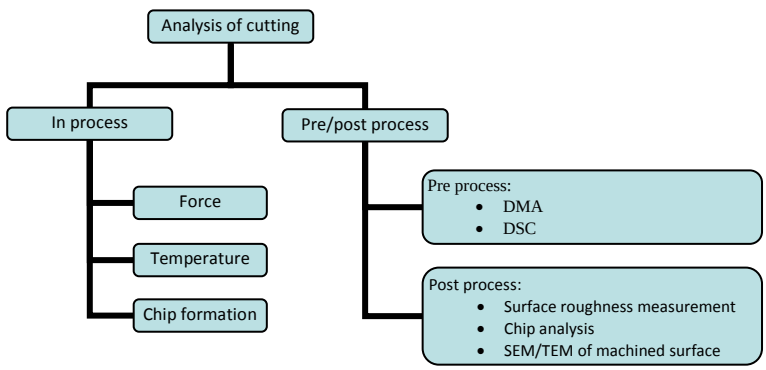

Figure 3: Experimental methodology for machining investigations on polymers

2.2 Force measurement

A dedicated force measurement solution was implemented using a Kistler type 9602 force sensor [19] mounted in a custom toolholder, as shown on the left in Figure 4. The Z axis of the sensor corresponds to the cutting force, and the resultant of the X and Y axes to the tangential force. A calibration curve for the X axis is shown on the right in Figure 4.

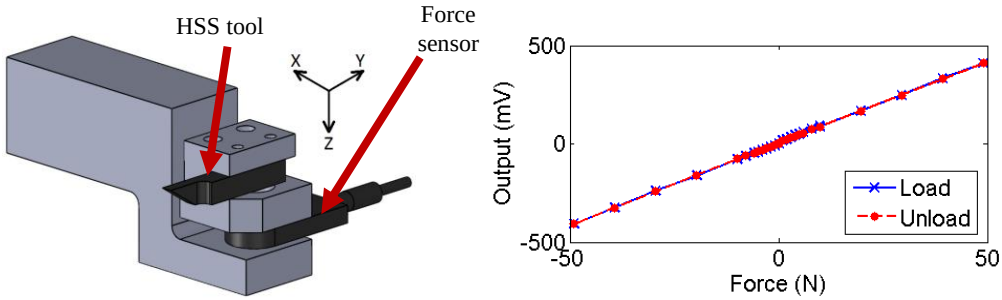

Figure 4: Custom toolholder (left), and sample force sensor calibration curve (right)

2.3 Temperature measurement

Tools were ground from High Speed Steel blanks, and a 1mm diameter hole was drilled in each to accommodate a K type thermocouple, as shown on the left in Figure 5. In addition, an IR temperature sensor [20] was placed to measure the temperature of the rake face of the tool, 20mm from the cutting edge. The spot size characteristic of the IR sensor is shown on the right in Figure 5.

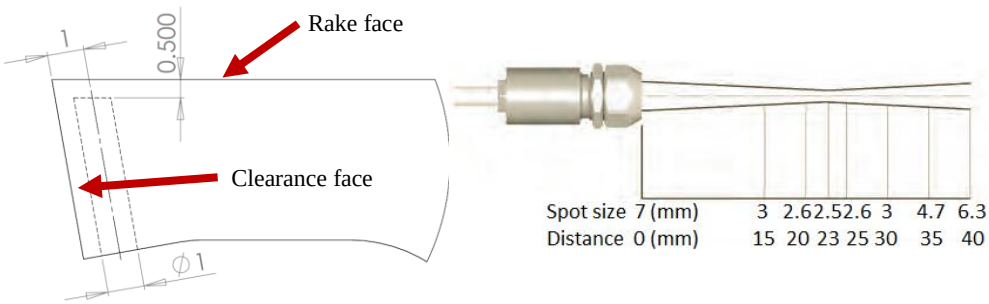

Figure 5: Thermocouple placement (left), and IR temperature sensor spot size (right)

2.4 High speed imaging

A Pixelink type 782 high speed camera [21] was mounted to the toolholder using a 3 axis linear stage to provide adjustment for position and focus of the picture. A Schott light source [22] was used to provide the lighting required for capture of high speed video.

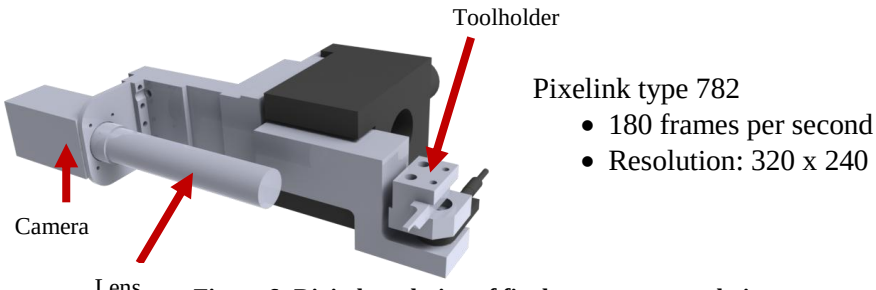

Figure 6: Digital rendering of final camera mount design

2.5 Workpiece design

Workpieces were designed as shown in Figure 7. In order to allow orthogonal cutting assumptions to be used, the workpieces were segmented into 2.2mm wide discs. It was found from preliminary testing that chip buildup caused the following problems:

1. Corruption of force data due to large amounts of chips sticking to the tool
2. Corruption of IR sensor data due to chips blocking the view of the sensor

As a result of these issues it was necessary to use segmented workpieces, as shown in Figure 8. The slot cut in the workpiece prevented the buildup of chips.

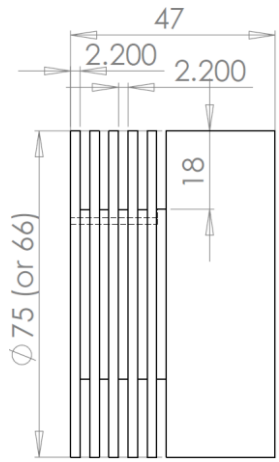

Figure 7: Workpiece design, showing discs

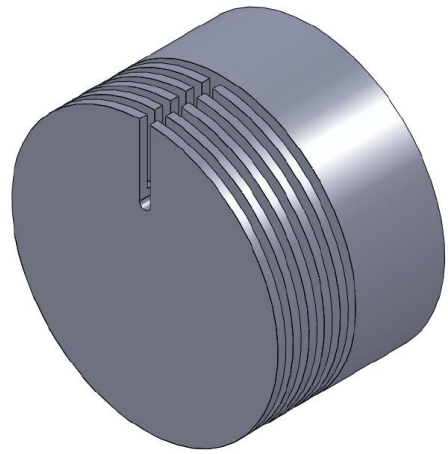

Figure 8: Slot cut in workpiece

2.6 Integration of measurement chain

Machining tests were carried out in an Okuma LT15-M. Data acquisition was carried out using a National Instruments CompactDAQ 9178 carrier [23], with analog input modules for voltage from the force sensor [24] and temperature from the thermocouple [25]. The complete in-process sensor suite is shown in Figure 9.

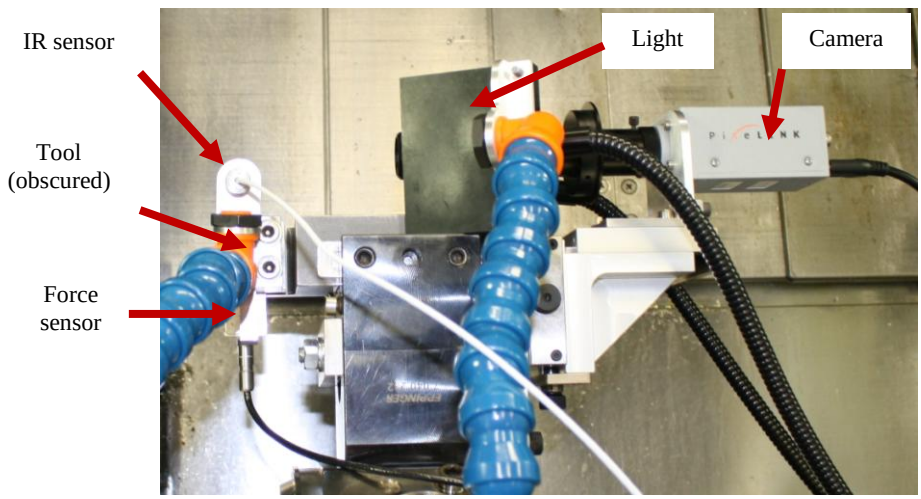

Figure 9: Sensor suite installed in Okuma LT15-M

After machining the surface roughness of the workpiece was measured using a Mitutoyo Surftest SJ400 portable surface roughness tester [26]. Tool sharpness and wear was checked both before and after machining using a Moticam 1000 [27] mounted on a toolmakers microscope, using a calibration slide and ImageJ software [28] to measure edge radius.

3. SAMPLE RESULTS

3.1 Force measurement

Sample force data from a machining operation with zero rake angle, cutting speed of 155 m/min, and depth of cut of 0.06 mm/rev are shown in Figure 10. High dynamic content is evident in both signals. A closer inspection of the data is also shown.

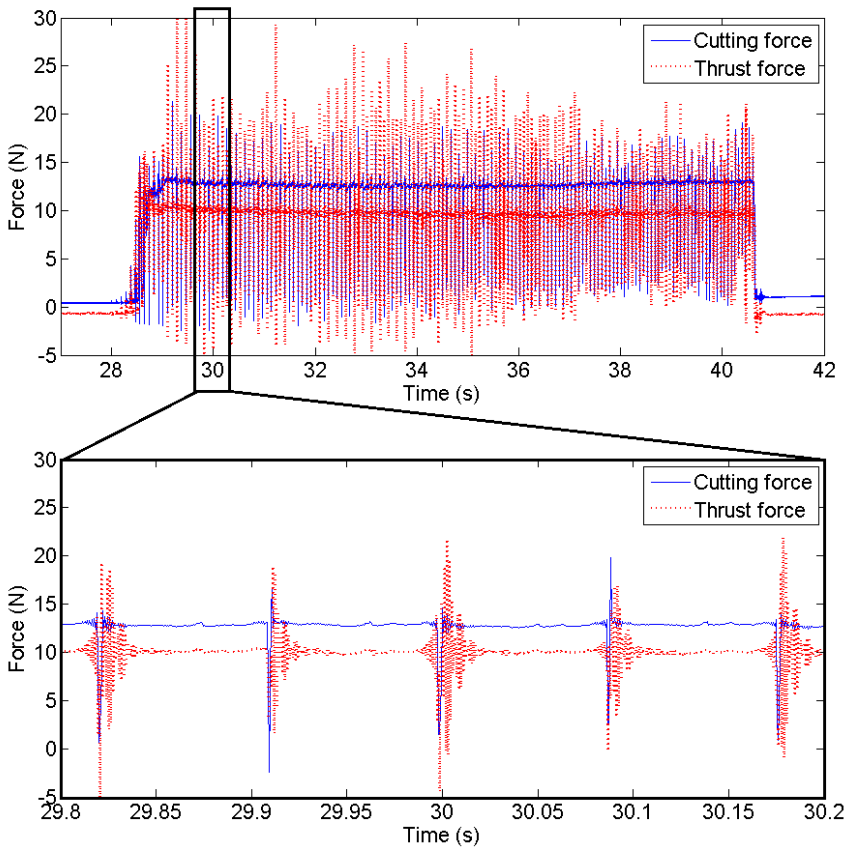

Figure 10: Raw data from polymer machining investigations

It is clear from this that the dynamic content is intermittent and cyclical, with peaks occurring at the same frequency as the rotation of the spindle, and caused by the slot cut in the workpiece to prevent chips from building up. There is also clear steady state behaviour of the cutting forces between the peaks. As the machining operations are carried out at constant surface speed, the spindle speed increases as the diameter decreases, and thus it is necessary to use a lowpass filter to remove the dynamic content and leave steady state cutting forces. A 10 Hz

lowpass filter was used, and experiments designed to avoid spindle speeds below 600 RPM. A filtered version of the data is shown in Figure 11.

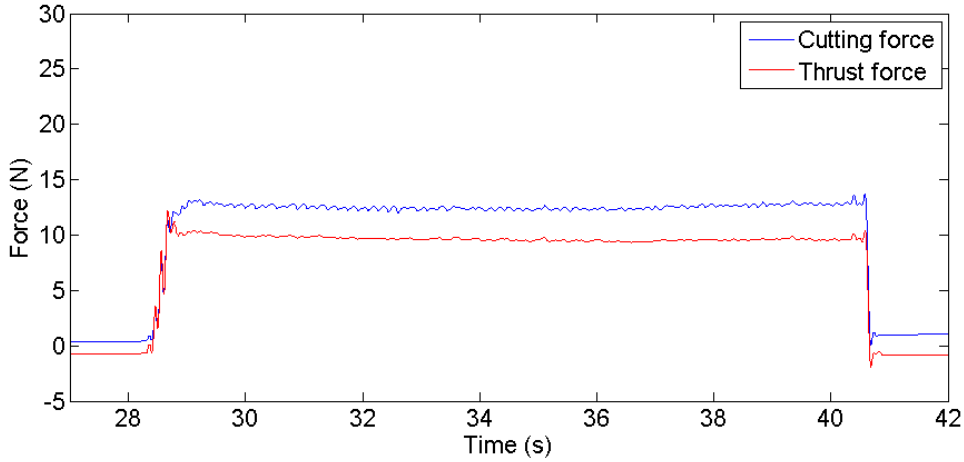

Figure 11: Filtered data of cutting force and thrust force

This data clearly illustrates steady state cutting forces, suitable for further analysis, and comparison with similar results for different machining conditions, tools, materials etc.

3.2 Temperature measurement

Sample temperature data from the same machining operation as shown above is shown in Figure 12.

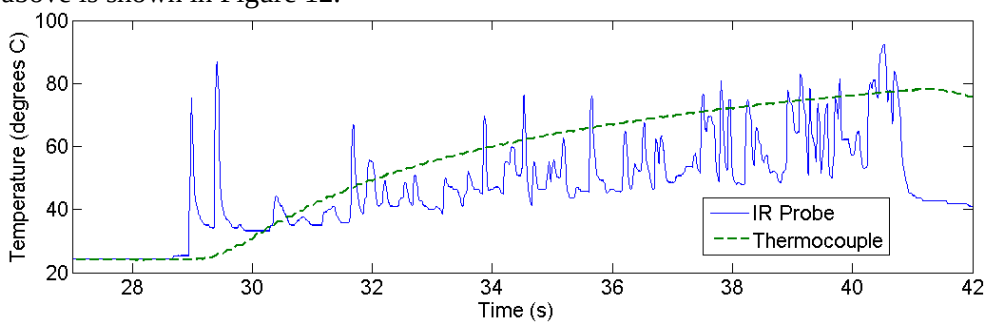

Figure 12: Temperature data from embedded thermocouple and IR probe

The thermocouple displays a lag of approximately one second, while the IR sensor shows a fast response, showing a spike in surface temperature quite soon after engagement. However, the IR sensor signal does not display reliable temperature data for the entire cutting operation, due to chips blocking the path of the beam. Further work is required to either redirect the chips away from the sensor, or to find another suitable location for temperature measurement during machining.

3.3 Chip analysis

Chips for 4 different sets of cutting conditions are shown in Figure 13. On the top left is an example of the chips from the machining operation shown in

Figures 10-12, while the remaining images show the changes in chip form as cutting speed and depth of cut are varied.

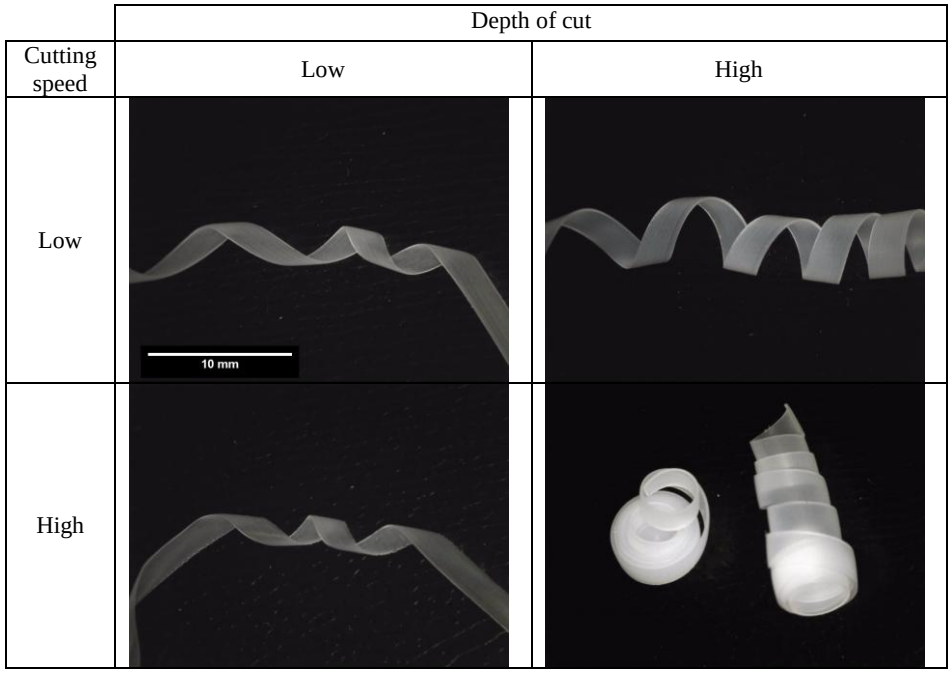

Figure 13: Chip analysis under various cutting parameters

It can be seen that the higher depth of cut delivers a thicker chip, as expected, but also displays a larger radius of curl.

3.4 High speed imaging

Sample frames from the video captured during machining are shown below

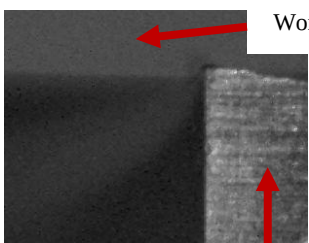

Figure 14

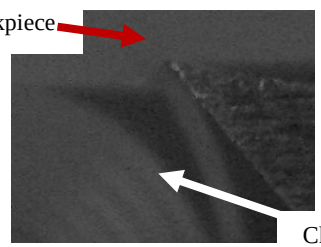

Figure 15

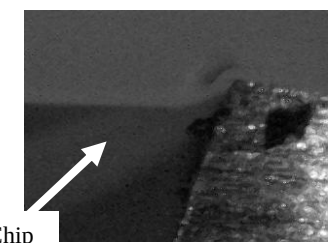

Figure 16

Figure 14 shows the cutting operation discussed previously, and shown in Figure 10. A thin chip is forming, which is blurred in this picture due to it curling away from the camera, out of focus. Figure 15 shows a cutting operation with a sharp, high rake angle tool, and a larger depth of cut. A thicker chip is evident, with a small radius of curl. Figure 16 shows a blunt, negative rake angle tool being used. This is an example of poor cutting conditions, as the workpiece is being highly distorted, and chips are discontinuous. These results are consistent with the findings of Kobayashi [2].

3.5 Surface roughness

Sample surface roughness results corresponding to the cutting conditions used for the chips shown top left in Figure 13 are shown in Table 2. The surface roughness measurement was repeated 5 times for each cutting operation, on different locations on the workpiece. Analysis using Minitab 16 [29] shows that depth of cut is a significant factor for surface roughness in this case ($P < 0.05$), with a higher depth of cut delivering lower surface roughness.

Cutting speed	Depth of cut	Mean (Ra)	Standard deviation
Low	Low	0.662	0.044
Low	High	0.572	0.077
High	Low	0.688	0.094
High	High	0.6	0.021

Table 2: Surface roughness results

4. CONCLUSION

A robust measurement chain has been developed which allows reliable, repeatable measurement of cutting forces, cutting temperatures, chip formation mechanisms and workpiece surface roughness. This measurement chain has been validated through the collection of sample data, and the analysis undertaken shows broad agreement with the work of Kobayashi. This measurement chain will facilitate future research into the machining of polymers.

ACKNOWLEDGEMENTS

The authors would like to acknowledge that this research has been carried out as part of a project funded by the Irish Research Council for Science, Engineering and Technology (IRCSET) and DePuy Ireland, with additional finance provided by the Department of Mechanical Engineering, Trinity College Dublin. Thanks must also be given to J.J. Ryan of the Department of Mechanical Engineering, Trinity College Dublin, for his assistance during testing.

5. REFERENCES

[1] Kurtz, S.M., *UHMWPE Biomaterials Handbook, Second Edition: Ultra High Molecular Weight Polyethylene in Total Joint Replacement and Medical Devices* 2009: Elsevier.

[2] Kobayashi, A., *Machining of plastics* 1967: McGraw-Hill.

[3] Kobayashi, A., Saito, K., *On the cutting mechanism of high polymers.* Journal of Polymer Science, 1962. **58**(166): p. 1377-1396.

[4] Kobayashi, A., Ohtani, N., Munemura, M., *Dynamic stress intensity factors during viscoelastic crack propagation at various strain rates.* Journal of Applied Polymer Science, 1980. **25**(12): p. 2789-2793.

[5] Kobayashi, A., Munemura, M., Ohtani, N., *Local disturbances preceding a running crack front in a viscoelastic solid.* Journal of Applied Polymer Science, 1981. **26**(7): p. 2147-2152.

[6] Kobayashi, A., Munemura, M., Ohtani, N., Suemasu, H., *Estimation of heat evolution during viscoelastic crack propagation by liquid crystal film technique.* Journal of Applied Polymer Science, 1982. **27**(10): p. 3763-3768.

[7] Kobayashi, A., Ohtani, N., *Initial slow crack growth behavior followed by rapid brittle fracture in a viscoelastic solid.* Journal of Applied Polymer Science, 1977. **21**(5): p. 1351-1358.
[8] Kobayashi, A., Ohtani, N., *Prefatigue hysteresis effects on viscoelastic crack propagation.* Journal of Applied Polymer Science, 1977. **21**(10): p. 2861-2866.
[9] Kobayashi, A., Ohtani, N., Sato, T., *Phenomenological aspects of viscoelastic crack propagation.* Journal of Applied Polymer Science, 1974. **18**(6): p. 1625-1638.
[10] Kobayashi, A., Sato, T., *Strain disturbances due to viscoelastic crack propagation.* Journal of Applied Polymer Science, 1974. **18**(7): p. 2039-2045.
[11] Kobayashi, A., Ohtani, N., Ino, S., *On creep test loading for soft polymers.* Journal of Applied Polymer Science, 1971. **15**(12): p. 3009-3013.
[12] Xiao, K.Q., Zhang, L.C., *The role of viscous deformation in the machining of polymers.* International Journal of Mechanical Sciences, 2002. **44**(11): p. 2317-2336.
[13] Carr, J.W., Feger, C., *Ultraprecision machining of polymers.* Precision Engineering, 1993. **15**(4): p. 221-237.
[14] Kobayashi, A., Ohtani, N., *Strain rate dependency on stress–strain relations of polypropylene.* Journal of Applied Polymer Science, 1971. **15**(4): p. 975-985.
[15] Fetecau, C., Stan, F., Munteanu, A., Popa, V., *Machining and surface integrity of polymeric materials.* International Journal of Material Forming, 2008. **1**(0): p. 515-518.
[16] Rubenstein, C., Storie, R.M., *The cutting of polymers.* International Journal of Machine Tool Design and Research, 1969. **9**(2): p. 117-130.
[17] Gindy, N.N.Z., *Critical Rake Angle And Cutting Forces Prediction In The Orthogonal Cutting Of Polymers.* International Journal of Production Research, 1988. **26**(9): p. 1535-1545.
[18] Teti, R., Jemielniak, K., O'Donnell, G., Dornfeld, D., *Advanced monitoring of machining operations.* CIRP Annals - Manufacturing Technology, 2010. **59**(2): p. 717-739.
[19] *Type 9602 Force Sensor With Integrated Electronics*. Kistler Instruments A.G. http://www.kistler.com/mediaaccess/9602A3_BP__000-173e-07.01.pdf (Accessed: 2/7/2012)
[20] *Data Sheet Optris CSMicro LT*. Optris GmbH. http://www.optris.com/tl_files/pdf/Downloads/Compact Series/Data Sheet optris CSmicro LT.pdf (Accessed: 2/7/2012)
[21] *Data Sheet, Pixelink 782 Series Firewire Camera*. Pixelink. http://www.pixelink.com/media/18356/datasheet_781&782.pdf (Accessed: 3/7/2012)
[22] *Data sheet, Schott ACE Remote Light Source*. Schott AG. http://www.schott.com/lightingimaging/english/download/01.22.10_ace_remote_row_.qxd.pdf (Accessed: 2/7/2012)
[23] *Data sheet, NI CompactDAQ USB Data Acquisition Systems*. National Instruments. http://sine.ni.com/ds/app/doc/p/id/ds-178/lang/en (Accessed: 3/7/2012)
[24] *Data Sheet, NI 9239 Analog Voltage Input Module*. National Instruments. http://sine.ni.com/nips/cds/view/p/lang/en/nid/203487 (Accessed: 3/7/2012)
[25] *Data Sheet, NI 9211 Thermocouple Input Module*. National Instruments. http://sine.ni.com/nips/cds/view/p/lang/en/nid/202554 (Accessed: 3/7/2012)
[26] *Data Sheet, Mitutoyo Surftest SJ400*. Mitytoyo America Corporation. http://www.mitutoyo.com/Images/003/308/2013_SJ-400.pdf (Accessed: 3/7/2012)
[27] *Specifications, Moticam 1000*. Motic. http://www.motic.com/ProductDetail.aspx?r=NA&lang=en&cid=&pid=14 (Accessed: 3/7/2012)
[28] *ImageJ website*. National Institutes of Health. http://rsbweb.nih.gov/ij/ (Accessed: 3/7/2012)
[29] *Minitab 16 Statistical Software*. Minitab Inc. http://www.minitab.com/en-GB/default.aspx (Accessed: 3/7/2012)